Wear 368-369 (2016) 379–389

Contents lists available at ScienceDirect

Wear

journal homepage: www.elsevier.com/locate/wear

Effect of Si and Al additions to carbon steel on material transfer and coating damage mechanism in turning with CVD coated tools

T. Aiso [a,*], U. Wiklund [a], M. Kubota [b], S. Jacobson [a]

[a] Tribomaterials group, The Ångström Laboratory, Uppsala University, Box 534, SE-751 21 Uppsala, Sweden
[b] Steel Research Laboratories, Nippon Steel & Sumitomo Metal Corporation, 1-8 Fuso-Cho, Amagasaki, Hyogo 660-0891, Japan

ARTICLE INFO

Article history:
Received 1 July 2016
Received in revised form
12 October 2016
Accepted 13 October 2016
Available online 15 October 2016

Keywords:
Steel
CVD coatings
Cutting tools
Transfer

ABSTRACT

Material transfer from the work materials to the tools strongly influences machining performance and tool life. The influence of Si and Al additions to carbon steel on the material transfer and coating wear in turning with CVD coated carbide tools is investigated. Three model steels are specifically designed to separately study the effects of the individual alloying elements: one reference steel with C as the only alloying element (Base steel), and two steels alloyed also with 1 mass% Si or Al. In the region around the depth of cut on the rake face, where the outside edge of the chip passes over the tool surface, the coating is worn mainly by abrasion when cutting the Base steel. When cutting the Si alloyed steel, an almost pure Si–O transfer layer covers the coating surface, which protects it from wear. When cutting the Al alloyed steel, an almost pure Al–O transfer layer forms on the coating. This layer promotes steel transfer and associated adhesive wear of the coating, which rapidly results in coating detachment and eventually causes notch wear. In the crater region, only the Al alloyed steel results in a transfer layer, an AlN layer that reduces the crater wear.

1. Introduction

Bars and wire rods of steels are widely used in structural components of the engine, drivetrain, suspension systems and other parts of automobiles. These steels undergo a variety of manufacturing processes, including e.g. forging, machining and heat treatment, when manufactured into the components. It was reported that the machining cost was more than 40% of the total manufacturing costs in some cases [1]. Thus, improving the machinability of the steel is an important possibility to reduce the cost of the manufactured components. Free-cutting additives, generally S and Pb, are often added to the steels to obtain good machinability. However, the use of high amounts of S is difficult, since this often results in reduced mechanical properties such as toughness and fatigue strength. Pb is an environmentally harmful substance and therefore its use is restricted, although it strongly enhances the machinability of steels without seriously deteriorating the mechanical properties. With this background, new knowledge and new techniques to improve the machinability are strongly needed.

One important phenomenon that strongly affects the machinability is the material transfer occurring during machining. Material transferred from the workpiece onto the cutting tool redefines the interface between the chip and the tool, and thereby its tribological properties. For example, through detailed analyses of the worn surfaces of gear hobs Gerth et al. [2] concluded that both tool wear and friction were reduced due to the formation of transfer layers on the tool rake face. Research has also been performed on how to control and take advantage of transfer layers [3–7].

The material transfer is very sensitive to the exact steel composition, and different alloying elements have very different effects. The complexity of most commercial steels makes systematic studies very difficult. Here, a simplified approach has been taken to allow systematic studies. Recently, the present authors have studied the effects of alloying element additions to workpiece steels on material transfer, friction characteristics and coating damage of a TiN coated tool [8–10]. In those studies, we have focused on the commonly used alloying elements Si, Mn, Cr and Al. To systematically study the individual roles of the alloying elements, model steels were carefully designed. These include one reference steel with 0.55 mass% C as the only alloying element and others alloyed also with 1 mass% Si, Mn, Cr or Al [8,9]. Using these steels, crossed cylinders sliding tests, simulating the contact between the chip and the tool in metal cutting, were carried out to achieve very well controlled conditions. The Si addition led to the formation of a continuous Fe–Si–O transfer layer on the tool coating, which reduced friction [8]. In contrast, the additions of Cr

* Corresponding author.
E-mail address: aiso.e88.toshiharu@jp.nssmc.com (T. Aiso).

http://dx.doi.org/10.1016/j.wear.2016.10.011
0043-1648/

Table 1
Chemical composition (mass%), hardness (HV) and heat treatment of the work materials.

	C	Si	Al	Mn	S	Hardness	Heat treatment
Base	0.55	0.003	0.003	< 0.001	0.001	196	1123 K/30 min – Oil quench → 763 K/300 min
Si	0.55	0.992	0.003	< 0.001	0.001	197	1223 K/30 min – Air cooling → 873 K/300 min
Al	0.55	0.003	1.010	0.001	0.001	206	1223 K/30 min – Oil quench → 843 K/300 min

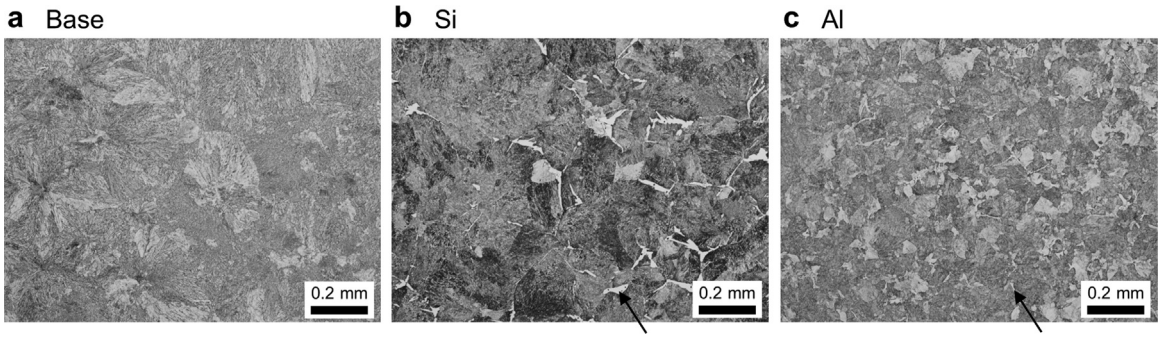

Fig. 1. Microstructure of the work materials. All steels mainly contained a fine pearlite microstructure. Small amounts of ferrite in the Si and Al alloyed steels are indicated by arrows.

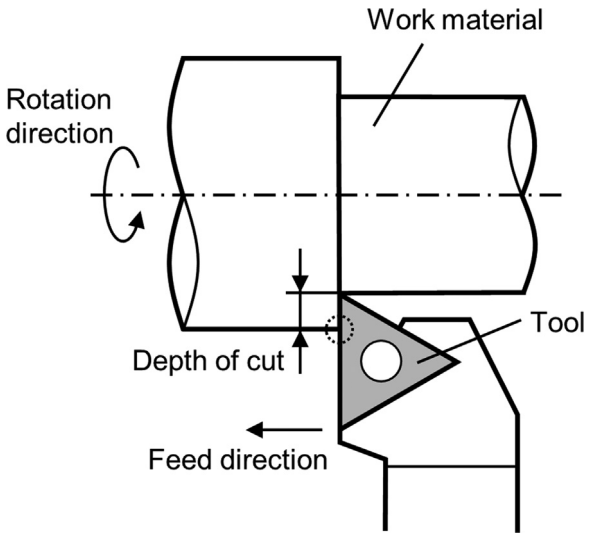

Fig. 2. Schematic illustration of the turning test. The region denoted "region of depth of cut" is indicated by a dashed circle.

Table 2
Cutting conditions.

Test parameter	
Cutting speed	250 m/min
Feed rate	0.3 mm/rev
Depth of cut	1.5 mm
Test duration	Up to 125 s
Lubrication	None (dry)

and Al resulted in Fe–Cr–O and Al–O layers, respectively [8,9]. Both layers caused higher friction and associated rapid coating fracture. The Mn addition resulted in the formation of a non-continuous Fe–Mn–O [9]. This non-continuous material did not protect the coating and thus the coating was worn mainly by abrasion. The effects of combined additions of these alloying elements were also studied, using the same types of model steels [10]. These findings clearly show that the alloying elements of Si, Mn, Cr and Al have decisive influence on the tribological properties at the chip/tool interface and thus also on the machinability of the respective steels.

The results in these recent studies [8–10] are expected to be relevant for milling, since the sliding test used has previously proven to be able to simulate the material transfer occurring during milling [11]. It is known that the type of cutting operation affects material transfer and tool damage mechanisms, often due to the large differences between continuous cuttings and intermittent cuttings such as turning and milling. The present work focuses on turning, and investigates the influence of Si and Al additions to the steel on material transfer and tool coating damage. The just mentioned model steels were used. As in our previous works, these were given similar microstructure and hardness by using heat treatment control [8,9]. This means the only significant difference was the chemical composition. CVD coated cemented carbide tools, which are commonly used in turning of steels, were used for the machining tests.

2. Material and methods

2.1. Work material

The steel work materials are identical to those used in our previous studies [8,9]. The same manufacturing processes and heat treatment cycles were employed (see Refs. [8,9] for details). The steels, used in the previous work and the present work, were not derived from the same charges, but only small variations in composition, microstructure and hardness were found. The Base steel included nominally 0.55 mass% C as the only alloying element, while the Si and Al alloyed steels also included nominally 1.0 mass% Si or Al, respectively, see Table 1. The different heat treatment cycles for each steel, shown in Table 1, were designed to minimize the differences in microstructure and hardness. The microstructure of all three steels was mainly fine pearlite, although some amount of tempered martensite was possibly contained in the Base steel, and small amounts of ferrite were present in the Si and Al alloyed steels, see Fig. 1. The hardness of all work materials was around 200 HV. Work material cylinders for the turning tests, with a diameter of 57 mm and a length of 230 mm, were cut out from the heat-treated steels.

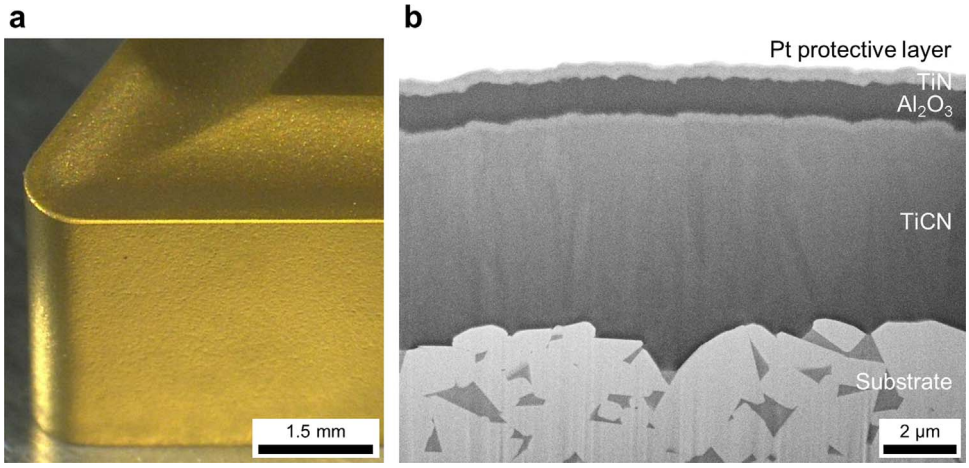

Fig. 3. (a) Appearance of an unused CVD coated carbide tool. (b) SEM image of a cross-section of the tool. The electron beam acceleration voltage was 10 kV and the cross-section was prepared using a focused ion beam.

Table 3
Average cutting forces for the Base steel, the Si alloyed steel and the Al alloyed steel, measured during 10 s of cutting. The differences compared to the Base steel are shown within brackets.

	Principal force [N]	Feed force [N]	Thrust force [N]	Resultant force [N]
Base	1002	460	290	1140
Si	1054 (+5.2%)	454 (−1.3%)	297 (+2.4%)	1185 (+3.9%)
Al	1048 (+4.6%)	468 (+1.7%)	312 (+7.6%)	1190 (+4.4%)

2.2. Turning test

The longitudinal turning tests, as shown in Fig. 2, were performed in a numerically controlled (NC) lathe, using the cutting conditions shown in Table 2. Here, the part of the tool cutting through the surface of the work material cylinder, indicated by the dashed circle in Fig. 2, is called the region of depth of cut. The cutting tools used for the tests were commercial CVD coated cemented carbide inserts for steel turning, TNMG160408, with a chip breaker as shown in Fig. 3a. The multilayer coating consisted of an about 7.2 μm TiCN inner layer, an about 1.2 μm Al_2O_3 intermediate layer and an about 0.6 μm TiN top layer, see Fig. 3b. The surface roughness, measured with white light interference profilometry, was Ra 0.64 ± 0.06 μm. For each steel, three separate tests were performed with different cutting times, 1, 10 and 125 s, to study the development of material transfer and wear. The cutting force was measured using a dynamometer during 10 s cutting tests for each steel. Chips were collected during the 10 s tests and their shapes were studied using optical microscopy. The 125 s tests were repeated twice and not much difference in material transfer and wear was observed using optical microscopy. Thus, the analyses for each test were performed with only one sample.

2.3. Analysis

Scanning electron microscopy (SEM), with an acceleration voltage of 10 or 15 kV, and energy dispersive X-ray spectroscopy (EDS) were used to study the tool surfaces. Focused ion beam (FIB) was employed to make cross-sections of the tools. Before preparing the FIB cross-section, a platinum deposition was performed on top of the tool to protect the surface from the subsequent ion polishing process. Cross-sections were analyzed using SEM and transmission electron microscopy (TEM) with the high-angle annular dark field (HAADF) technique at an acceleration voltage of 300 kV.

3. Results

3.1. Cutting force and chip shape

The three force components, called principal force, feed force and thrust force, and the resultant force are presented in Table 3. For all three steels, each cutting force component was almost constant during the 10 s test and thus the average values are shown. The force components were almost at the same level for the three steels, resulting in less than 5% difference in resultant force.

The chips from the three steels showed similar shapes, see Fig. 4. All chips were discontinuous, broken to short roll segments. This shape is generally considered to be ideal to avoid excess load on the cutting edges.

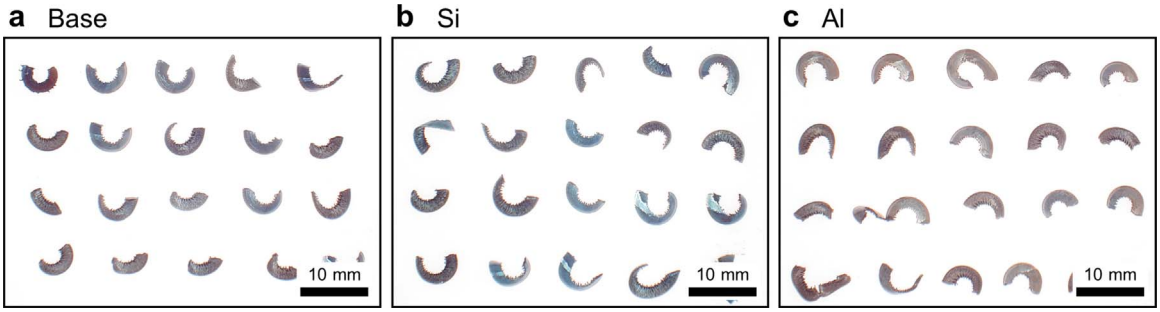

Fig. 4. Representative chips from the Base steel, the Si alloyed steel and the Al alloyed steel collected during 10 s cutting tests and shown without particular order.

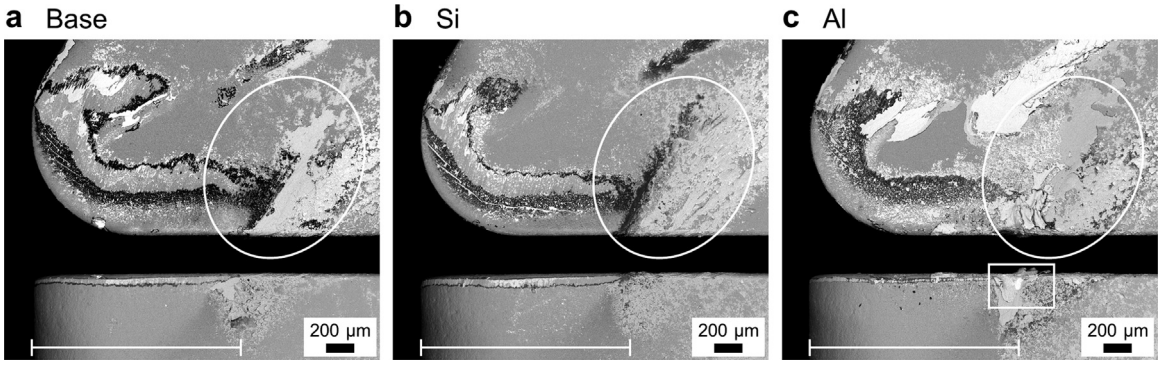

Fig. 5. Backscattered electron images of the rake faces and flank faces of the tools after cutting (a) the Base steel, (b) the Si alloyed steel and (c) the Al alloyed steel for 125 s. The area in the white rectangle is magnified in Fig. 7. The white bars in the lower parts of the images show the depth of cut, i.e. 1.5 mm. The white ovals indicate the region of the depth of cut, where most material transferred. The electron beam acceleration voltage was 15 kV.

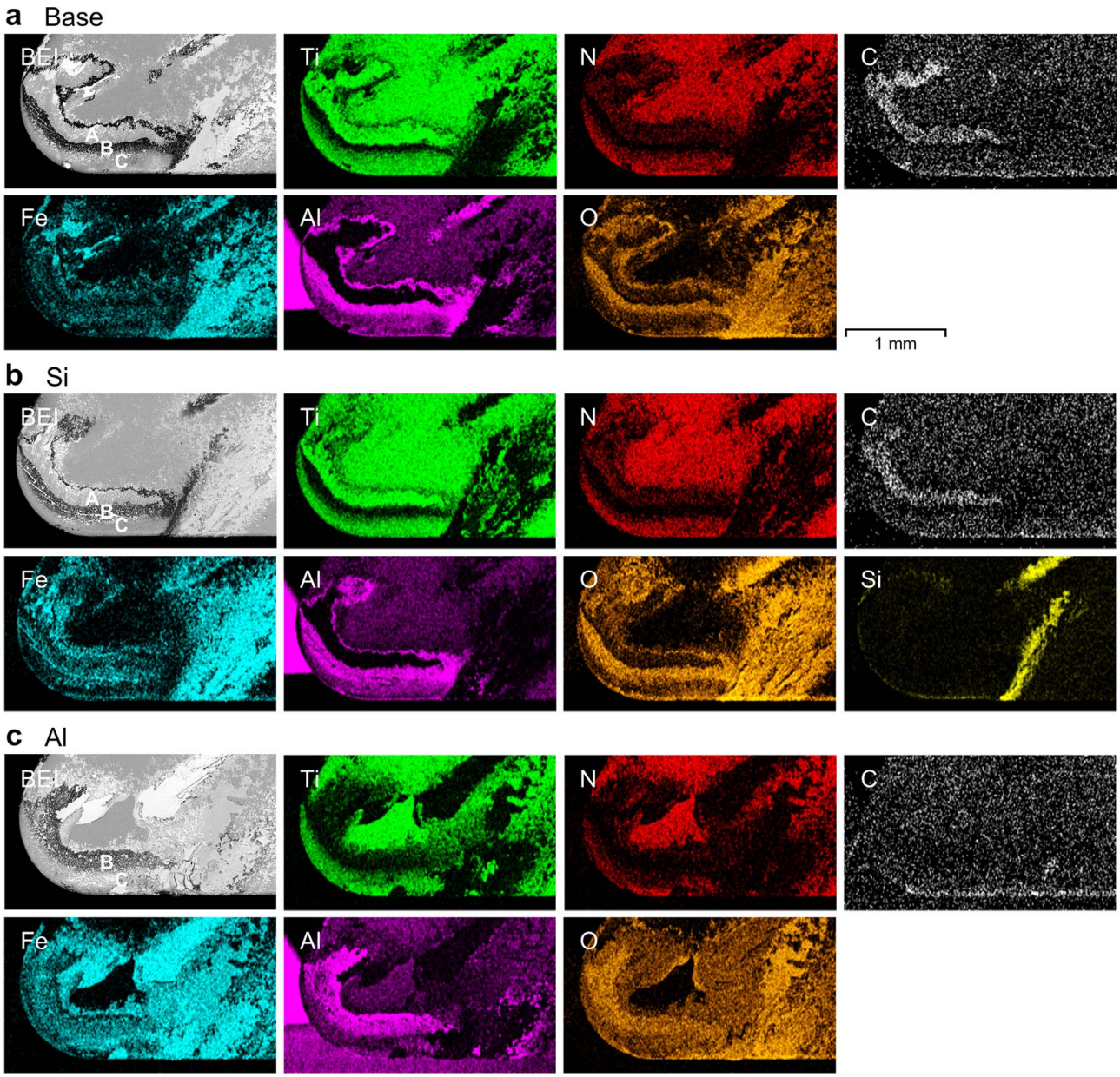

Fig. 6. Backscattered electron images (BEI) and EDS maps of the rake faces after cutting (a) the Base steel, (b) the Si alloyed steel and (c) the Al alloyed steel for 125 s. A, B and C in the backscattered electron images indicate regions of exposed TiCN, exposed Al_2O_3 and TiN, respectively. The electron beam acceleration voltage was 15 kV.

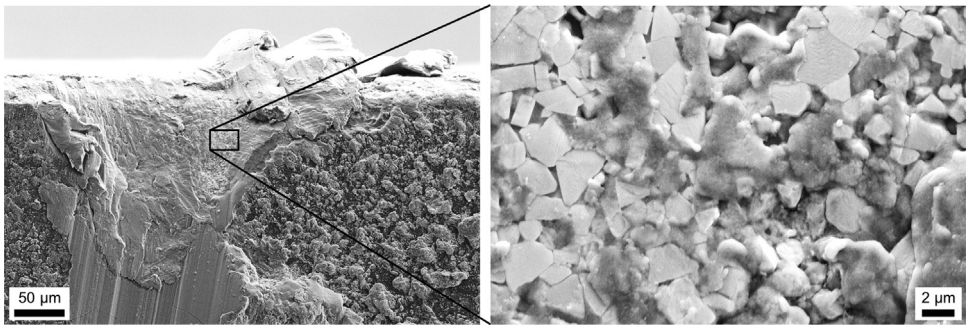

Fig. 7. SEM images of the notch wear area on the flank face after cutting the Al alloyed steel for 125 s. An overview image, corresponding to the white rectangle in Fig. 5, is shown to the left and the area in the black rectangle is magnified in the image to the right. The electron beam acceleration voltage was 15 kV.

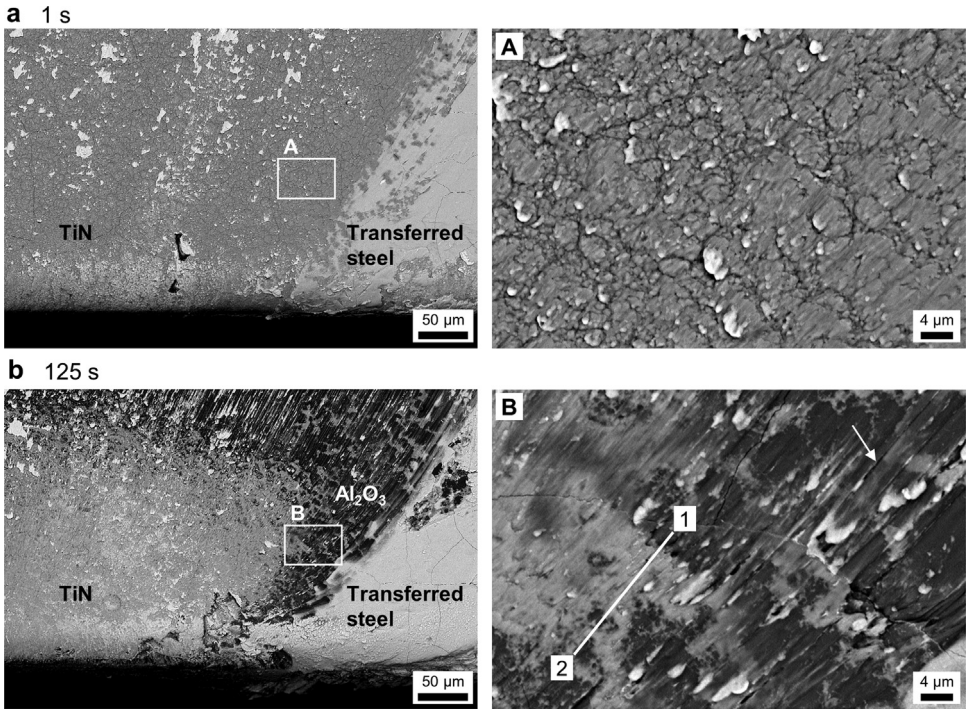

Fig. 8. Backscattered electron images of the rake faces in the region of the depth of cut after cutting the Base steel for (a) 1 s and (b) 125 s. Overview images are shown to the left and the areas within the white rectangles A and B are magnified in the images to the right. The white line between the numbers 1 and 2 indicates the position of the cross-section in Fig. 9. A typical groove formed on the tool surface is indicated by the arrow. The electron beam acceleration voltage was 15 kV.

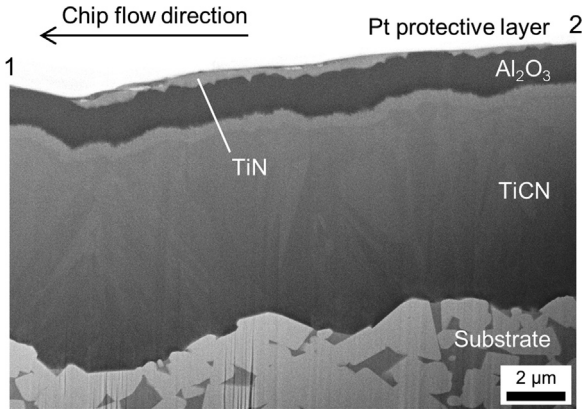

Fig. 9. SEM image of a FIB cross-section of the worn rake face in the region of the depth of cut after cutting the Base steel for 125 s. The cross-section was obtained at the position of the white line between the numbers 1 and 2 in Fig. 8. The electron beam acceleration voltage was 10 kV.

3.2. *Surface appearance of the cutting tools*

After cutting for 125 s, the three work material steels resulted in clear differences in material transfer and tool wear, see Fig. 5. Material transfer occurred mainly around the region of the depth of cut on the rake face, encircled in Fig. 5, where the outside edge of the chip passed over the tool surface. In this region, oxidized transferred steel was found for all three steels, see Figs. 5 and 6. The amounts of transferred steel were similar for the Base steel and the Si alloyed steel, while much more transferred steel was seen for the Al alloyed steel. The Al alloyed steel also displayed the striking notch wear indicated by the white rectangle in Fig. 5. In the notch wear region, the coating was worn and the substrate was exposed, see Fig. 7. For the Si alloyed steel, Si-rich transferred material had formed inside the oxidized transferred steel, see Fig. 6.

The Base steel and the Si alloyed steel showed similar crater wear on the rake face, having distinct gray regions with black rims in SEM, see Fig. 5. The EDS maps in Fig. 6 revealed that these gray and black areas, indicated by A and B, correspond to exposed TiCN and exposed Al_2O_3, respectively. In contrast, the Al alloyed steel

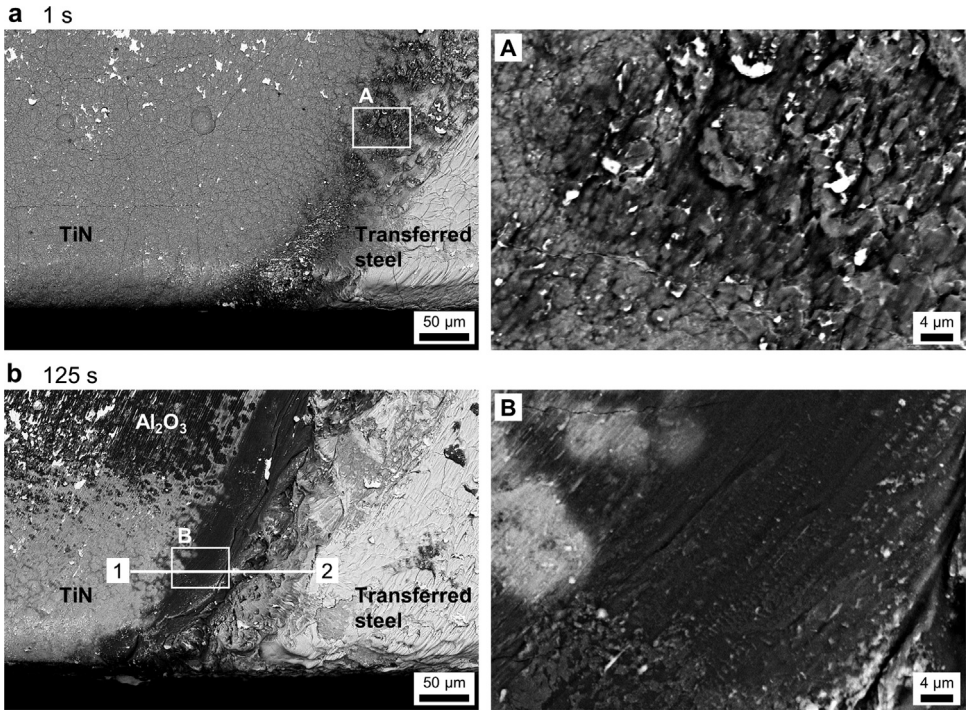

Fig. 10. Backscattered electron images of the rake faces in the region of the depth of cut after cutting the Si alloyed steel for (a) 1 s and (b) 125 s. Overview images are shown to the left and the areas within the white rectangles A and B are magnified in the images to the right. The white line between the numbers 1 and 2 indicates the position of the cross-section in Fig. 11. The electron beam acceleration voltage was 15 kV.

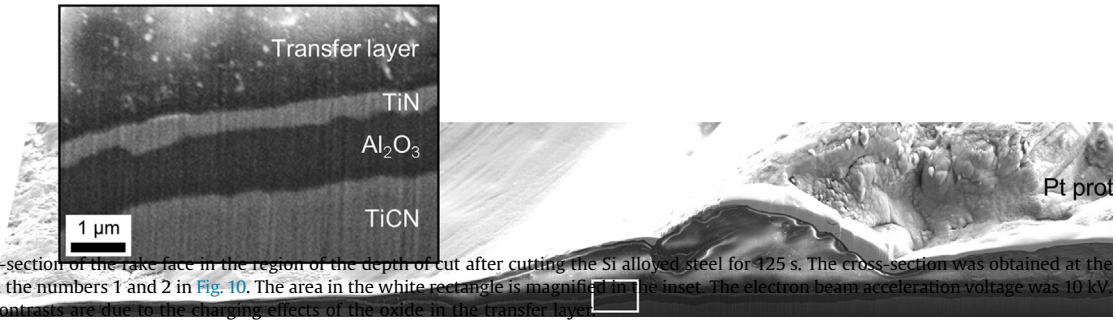

Fig. 11. SEM images of a FIB cross-section of the rake face in the region of the depth of cut after cutting the Si alloyed steel for 125 s. The cross-section was obtained at the position of the white line between the numbers 1 and 2 in Fig. 10. The area in the white rectangle is magnified in the inset. The electron beam acceleration voltage was 10 kV. Please note that the very bright contrasts are due to the charging effects of the oxide in the transfer layer.

showed smaller crater wear as only Al_2O_3, not TiCN, was exposed, see Figs. 5 and 6.

3.3. Material transfer and wear of the cutting tools in the region of depth of cut

3.3.1. Transfer and wear when cutting the Base steel

Apart from the large amount of oxidized transferred steel in the outer region of the chip/tool contact, only a small amount of transferred steel, and almost no wear, was found after cutting the Base steel for 1 s, see Fig. 8a. This steel transfer tended to be initiated at the surface roughness of the coating. After 125 s, the TiN top layer of the coating was worn and the Al_2O_3 was exposed, see Fig. 8b. Only in the region within the white rectangle in Fig. 8b the wear scar extended all the way to the cutting edge. The magnified detail in Fig. 8b shows some grooves formed along the chip flow direction, as indicated by the arrow. The FIB cross-section in Fig. 9, obtained in this worn region, reveals a smooth surface of the TiN layer, which indicates the coating has been gradually worn down in thickness. Notably, this wear process without apparent fractures is evidenced even in places where the TiN layer is almost fully removed from the Al_2O_3 layer. Please note that the narrow cracks visible in Fig. 8b were formed during the coating deposition process and thus existed before the cutting tests.

3.3.2. Transfer and wear when cutting the Si alloyed steel

Already after cutting the Si alloyed steel for 1 s, a dark region had formed inside the region with oxidized transferred steel, see Fig. 10a. This region corresponds to where the wear of the TiN layer occurred with the Base steel in Fig. 8. However, with the Si alloyed steel the dark shade is not due to exposed Al_2O_3 but a result of a transfer layer. This transfer layer had grown thicker and continuous after a cutting time of 125 s, see Fig. 10b. The transfer layer showed a relatively smooth surface. The FIB cross-section of the tool, shown in Fig. 11, verified that the transfer layer continuously covered almost all the coating surface in this region and allowed its maximum thickness to be measured to approximately 16 µm. Underneath the transfer layer, the coating thickness was almost intact. The TEM study revealed that most of the transfer layer was almost pure Si–O, see Fig. 12. The layer also contained small amounts of Fe, seen as small bright circular features in the image. Selected area diffraction, obtained from an area about 1 µm in diameter, resulted in a halo pattern, proving the Si–O transfer layer to be amorphous.

3.3.3. Transfer and wear when cutting the Al alloyed steel

Already after 1 s, drastic transfer and wear occurred when cutting the Al alloyed steel, see Fig. 13. Apart from the oxidized transferred steel in the outer region of the chip/tool contact, a

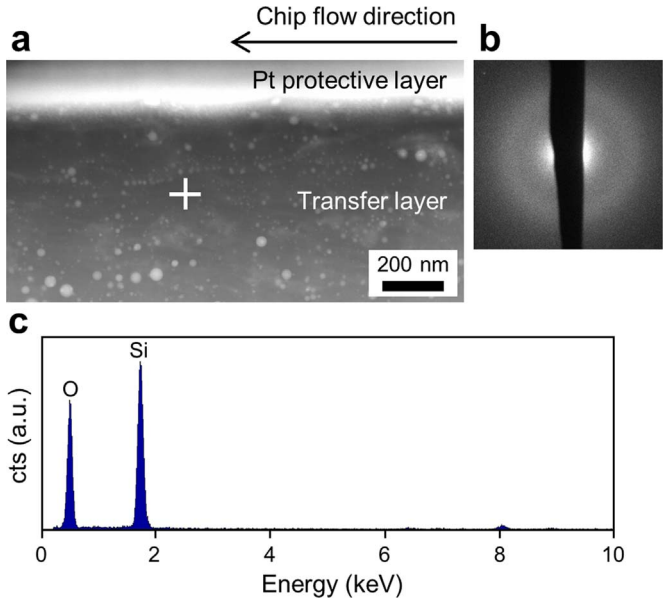

Fig. 12. (a) HAADF-STEM image of a FIB cross-section of the transfer layer on the rake face in the region of the depth of cut after cutting the Si alloyed steel for 125 s. (b) Selected area diffraction pattern obtained from an area about 1 μm in diameter. (c) EDS spectrum obtained at the position indicated by the white cross.

large amount of steel transferred also to the inner region, as shown in the overview image and the magnified image of area A in Fig. 13a. A TEM cross-section obtained from area A revealed that an almost pure Al–O transfer layer, about 100 nm thick, was covering the TiN top layer surface, see Fig. 14. On top of and in front of this Al–O transfer layer, metallic and oxidized steel was attached.

Closer to the cutting edge, in area B in Fig. 13a, the coating had fractured and parts of it had been removed. A cross-section image of this region, see Fig. 15a, revealed that all three sub-layers of the coating were worn. The TiN and Al_2O_3 layers were partially worn off, leaving the TiCN exposed to wear. The worn coating had an irregular surface, very different from the relatively smooth surface of the coating worn against the Base steel (Fig. 9). Transferred steel was attached to the worn coating. At the cutting edge, i.e. in area C in Fig. 13a, the coating was locally worn away, leaving a few WC grains of the substrate exposed, seen as the very bright parts in the image.

After 10 s cutting, the region with exposed substrate had expanded, including the region where the coating was partially detached after 1 s cutting, see Fig. 13b. Transferred steel covered parts of the exposed substrate surface as in area D. In the border region between exposed substrate and remaining coating a large crack had been generated, parallel to the chip flow direction, see Fig. 15b. Somewhat guided by the interface between the TiCN layer and the substrate, the crack had sometimes grown through the TiCN and sometimes through WC grains in the substrate. Transferred steel had both penetrated into the crack and partially covered the surface of the worn coating.

3.4. *Material transfer and crater wear of the cutting tools*

After 125 s cutting, the Base steel and the Si alloyed steel had caused similar widths of the crater wear of the coating, while the Al alloyed steel had caused a narrower crater, see Fig. 16. In addition, the rims of the craters had different appearances as shown in Fig. 17. After cutting the Base steel and the Si alloyed steel, only the coating components and the transferred steel were seen. In contrast, with the Al alloyed steel, a transfer layer containing Al and N was detected. The TEM cross-section in Fig. 18 showed that this transfer layer was approximately 400 nm thick and the thickness of the TiN layer underneath was almost intact, about 400–600 nm. The transfer layer consisted of a mixture of AlN and transferred metallic steel.

4. Discussion

The experimental results demonstrate that alloying element additions of 1 mass% significantly influence the material transfer and wear of the coating in turning. The test condition with the three model steels having similar microstructure and hardness resulted in similar cutting forces and chip shapes, c.f. Table 3 and Fig. 4. This means that in the present study the coating damage mechanisms are mainly due to the material transfer behavior, almost without influences from differences in the cutting force and chip shape. The three model steels exhibited huge differences in the transfer and wear even after 1 s cutting, c.f. Figs. 8, 10 and 13. It was shown also in our previous studies using sliding tests [8–10] that material transfer initiated extremely fast, less than 0.025 s, and characteristic transfer layers developed in the first few seconds. Together, these results emphasize the importance of the present controlled studies focusing on the very initial stage to understand the mechanisms of material transfer and closely associated coating wear.

In turning, the major part of chip/tool contact on the rake face is within the seizure region, i.e. not sliding, and there is virtually no oxygen supply from the atmosphere [12]. On the other hand, in the region of the depth of cut, where the chip edge moves over the tool surface, sliding occurs either intermittently or continuously [12]. This contact condition allows some oxygen from the atmosphere to access the contacting surfaces [12]. Moreover, oxygen also enters this specific region as a thin oxide present on the surface of the work material, c.f. Fig. 2. These facts explain the oxidized steel transferred around the region of the depth of cut for all three steels.

When cutting the Base steel, the TiN layer was worn around the region of the depth of cut, c.f. Fig. 8b. The grooves on the worn surface shown in Fig. 8b suggest that abrasion caused by hard inclusions, such as aluminium oxides, in the steel was one of the main wear mechanisms, although other wear mechanisms, such as diffusion wear and superficial plastic deformation of the coating, might also be involved.

When cutting the Si alloyed steel, an almost pure Si–O transfer layer was formed at the position corresponding to the worn region when cutting the Base steel, c.f. Figs. 10 and 12. Si is known to oxidize more easily than Fe [13]. Therefore, in the region with limited oxygen supply only Si but not Fe becomes oxidized, resulting in the formation of the almost pure Si–O. This Si–O layer was continuously covering the coating, protecting it from wear, c.f. Fig. 11.

When cutting the Al alloyed steel, an almost pure Al–O transfer layer was formed in the corresponding region, c.f. Figs. 13 and 14. Since Al is even more easily oxidized than Si [13], the formation of the almost pure Al–O was explained as in the case of the almost pure Si–O. All steels resulted in oxidized transferred steel in the outer region of the chip/tool contact, but the Al alloyed steel also resulted in a large amount of steel transferred around the region of the depth of cut, on top of and in front of the Al–O layer, c.f. Figs. 13a and 14. This suggests that the Al–O layer promoted the steel transfer. This behavior can be explained by the same mechanism suggested by the present authors for sliding tests [9], that the roughness of the already transferred Al–O encourages steel transfer. Interestingly, this roughness induced transfer was not present on the Si–O layer. This is probably mainly due to the smoother surface appearance of the Si–O layer, c.f. Fig. 10. The fact

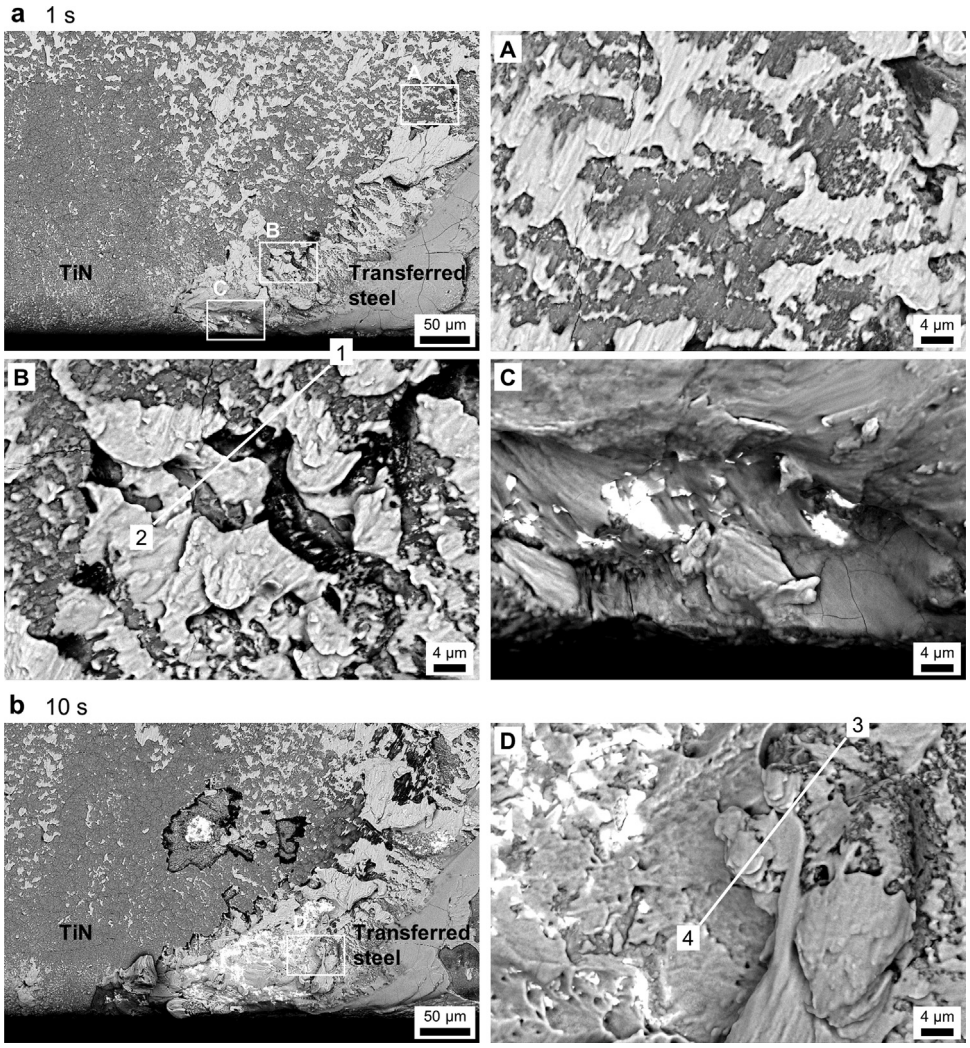

Fig. 13. Backscattered electron images of the rake faces in the region of the depth of cut after cutting the Al alloyed steel for (a) 1 s and (b) 10 s. Overview images are shown to the upper left in (a) and the left in (b), and the areas within the white rectangles A, B, C and D are magnified in the other images. The white lines, between the numbers 1 and 2 in area B and between the numbers 3 and 4 in area D, indicate the positions of cross-sections in Fig. 15. The electron beam acceleration voltage was 15 kV.

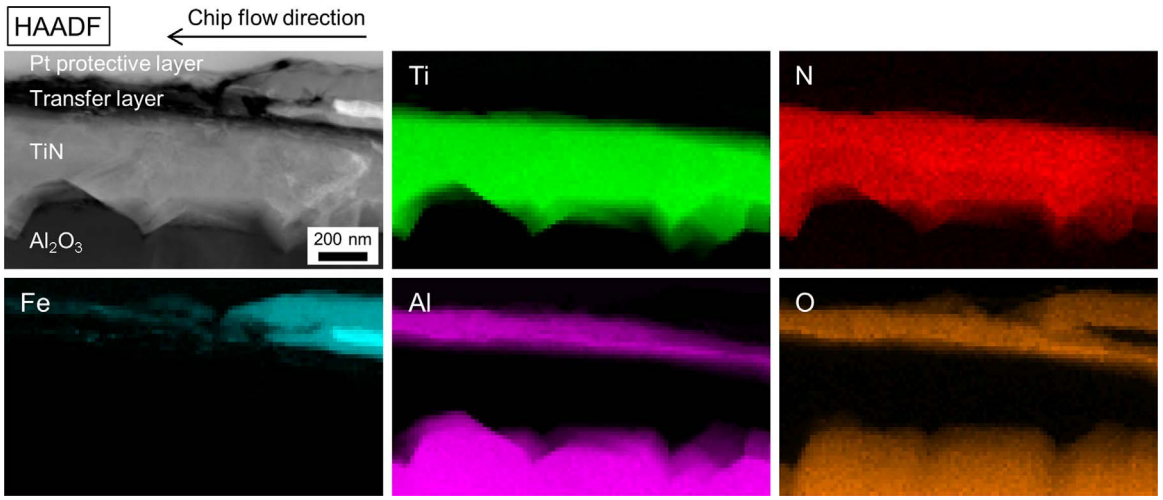

Fig. 14. HAADF-STEM image and EDS maps of a cross-section of the surface on the rake face in the region of the depth of cut after cutting the Al alloyed steel for 1 s. The cross-section was made in area A in Fig. 13a.

that the Si–O layer was amorphous, c.f. Fig. 12, implies that the temperature had been very high during cutting so that the layer could deform and become smooth. The Si–O has a lower melting point than the Al–O; 1996 K for the Si–O [14] and 2323 K for the Al–O [15]. This difference suggests the two oxides have different tendencies to soften in the contact. Presumably, this results in the

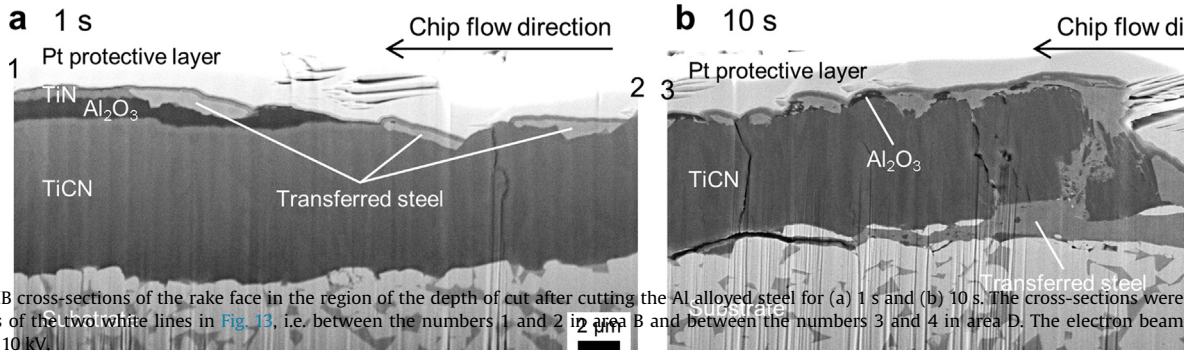

Fig. 15. SEM images of FIB cross-sections of the rake face in the region of the depth of cut after cutting the Al alloyed steel for (a) 1 s and (b) 10 s. The cross-sections were obtained at the positions of the two white lines in Fig. 13, i.e. between the numbers 1 and 2 in area B and between the numbers 3 and 4 in area D. The electron beam acceleration voltage was 10 kV.

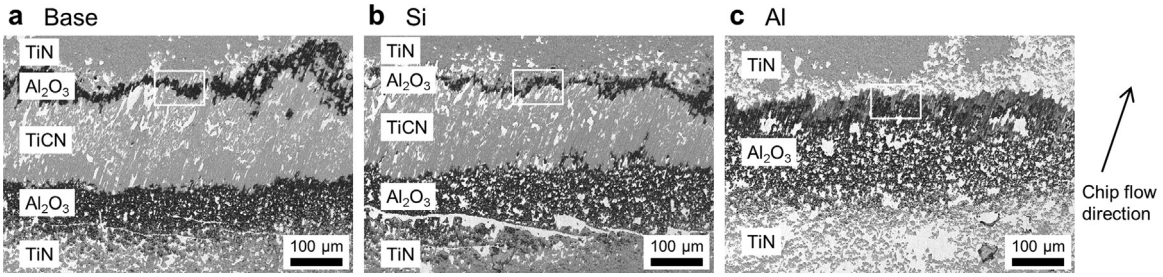

Fig. 16. Backscattered electron images of the crater wear regions after cutting (a) the Base steel, (b) the Si alloyed steel and (c) the Al alloyed steel for 125 s. The white rectangles are magnified in Fig. 17. The electron beam acceleration voltage was 15 kV.

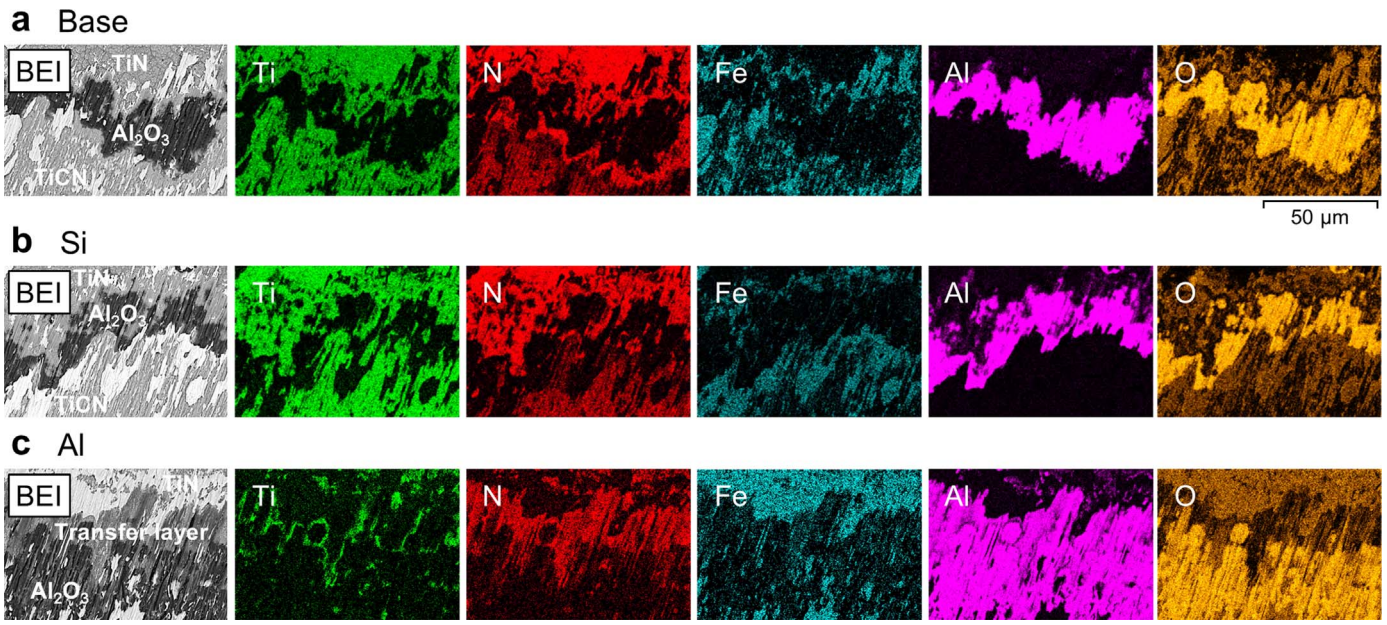

Fig. 17. Backscattered electron images (BEI) and EDS maps of the crater wear regions after cutting (a) the Base steel, (b) the Si alloyed steel and (c) the Al alloyed steel for 125 s. The regions are marked with white rectangles in Fig. 16. The electron beam acceleration voltages for SEM imaging and EDS analysis were 15 kV and 10 kV, respectively.

different surface topographies, and hence the different tendencies to steel transfer. These results are similar to those in our previous studies on transfer in sliding contacts [8,10], showing that the Si-rich transfer layers, mainly containing Si–O and Fe–Si–O, were associated to low friction and a smooth surface appearance.

The intense steel transfer when cutting the Al alloyed steel promoted adhesive wear of the coating and the substrate. The very uneven worn surface of the coating in Fig. 15a indicates that parts of the coating became detached together with transferred steel and subsequently transported away by the chip flow. This adhesive wear proceeded quickly, as large parts of coating and substrate were removed within 10 s, c.f. Fig. 15b. This wear process eventually caused the large notch wear shown in Fig. 7.

The surface roughness of the coating influenced material transfer behavior to some extent, see e.g. Fig. 8a. However, the large differences in transfer and coating wear between three steels, using the same type of tools, mean that in this study the steel compositions were more important for the transfer and wear than the coating surface roughness.

In the crater regions, where there is no oxygen supply, no oxide layer was formed with any of the three steels. With the Base steel and the Si alloyed steel only isolated spots of transferred steel were found, c.f. Fig. 16. However, cutting the Al alloyed steel resulted in the formation of a transfer layer containing Al and N, c.f. Figs. 16–18. Tanaka et al. [3] suggested that the presence of an AlN transfer layer on the rake face reduced the diffusion between the

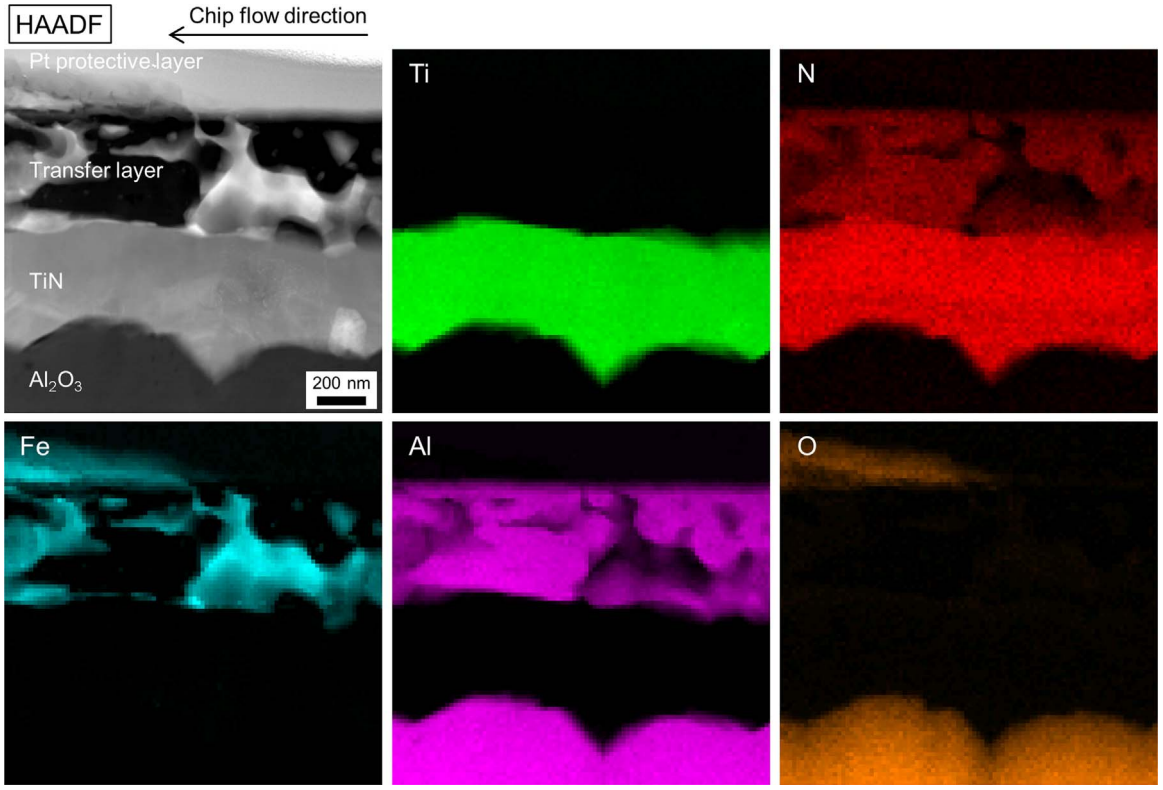

Fig. 18. HAADF-STEM image and EDS maps of a cross-section of the transfer layer in the crater wear region after cutting the Al alloyed steel for 125 s. The cross-section was made in the area shown in Fig. 17c.

chip and the tool. Here, this mechanism probably explains the smaller crater wear with the Al alloyed steel.Figure 18 shows that an AlN transfer layer existed also on the transferred steel, not only on the TiN, which likely implies that the N in AlN was not supplied from the tool coating but from the steel. The contents of AlN precipitates in the steels were measured and proved to be very similar for the three steels; 0.0028, 0.0025, 0.0024 mass% for the Base steel, the Si alloyed steel and the Al alloyed steel, respectively. This means that the AlN transfer layer on the rake face cannot be formed from the precipitates, since it formed only when cutting the Al alloyed steel. Yaguchi et al. [16] concluded that Al and N in solid solution can react and form an AlN transfer layer at the chip/tool interface because of the high heat generation during cutting. In the present work, all three steels contained about 0.0009 mass% N, where most N was contained in the AlN precipitates. Therefore, the amount of N in solid solution is believed to be very small. Despite this, the abundance of Al in solid solution in the Al alloyed steel might, at high temperatures, allow Al to react with the small amount of N in solid solution. Revealing the details of this mechanism would need further studies, using steels with highly controlled Al and N contents.

The results in this work are important for both turning and milling. In milling, where the tool repeatedly undergoes short term contact with the work material followed by a period out of contact, oxygen is intermittently supplied to all parts of the rake face, which makes the oxides dominate [2]. Turning, where the tool is in continuous contact and there is only limited oxygen supply, allows different regions to develop; one oxygen deficient and one dominated by oxides. The choice of turning for this work thus allowed different phenomena to be studied separately, phenomena that are more or less present in various forms of cutting operations.

5. Conclusions

The present investigation clearly demonstrates that within seconds of cutting, alloying element additions of 1 mass% significantly influence the material transfer and therefore immediately control the wear of the tool coating in turning of steel. Further, it clearly demonstrates that different alloying elements lead to different wear and transfer mechanisms, in some cases protecting the coating and in others intensifying the wear. The investigation of the individual roles of two different alloying elements was made possible by the design of three model steels; Fe–0.55C (Base steel), Fe–0.55C–1Si (Si alloyed steel) and Fe–0.55C–1Al (Al alloyed steel) in mass%. A commercial CVD coated cemented carbide tool was selected for the turnings tests.

In the region around the depth of cut, where oxygen is present, the coating was worn mainly by abrasion when cutting the Base steel. When cutting the Si alloyed steel, an almost pure Si–O transfer layer covered the coating surface and protected it from wear. When cutting the Al alloyed steel, an almost pure Al–O transfer layer was formed on the coating, and steel tended to transfer on top of and in front of this layer. This transferred steel promoted adhesive wear of the coating, which rapidly resulted in coating detachment and eventually led to notch wear.

In the crater wear region, where virtually no oxygen is present, a transfer layer formed only when cutting the Al alloyed steel. This layer, containing Al and N, led to less crater wear when cutting the Al alloyed steel than when cutting either the Base steel or the Si alloyed steel.

Acknowledgement

Mr. Kei Miyanishi, Nippon Steel & Sumitomo Metal Corporation, is acknowledged for assistance with the turning test. Financial

support from Nippon Steel & Sumitomo Metal Corporation is acknowledged.

References

[1] H.K. Tönshoff, C. Stanske, Material aspects in machining of forged parts, in: Proceedings of the international conference on high productivity machining, materials and processing, 1985, pp. 207–222.
[2] J. Gerth, M. Larsson, U. Wiklund, F. Riddar, S. Hogmark, On the wear of PVD-coated HSS hobs in dry gear cutting, Wear 266 (2009) 444–452.
[3] R. Tanaka, Y. Yamane, K. Sekiya, N. Narutaki, T. Shiraga, Machinability of BN free-machining steel in turning, Int. J. Mach. Tools Manuf. 47 (2007) 1971–1977.
[4] N. Matsui, K. Watari, Wear reduction of carbide tools observed in cutting Ca-added steels for machine structural use, ISIJ Int. 46 (2006) 1720–1727.
[5] J. Kümmel, J. Gibmeier, E. Müller, R. Schneider, V. Schulze, A. Wanner, Detailed analysis of microstructure of intentionally formed built-up edges for improving wear behaviour in dry metal cutting process of steel, Wear 311 (2014) 21–30.
[6] J. Kümmel, D. Braun, J. Gibmeier, J. Schneider, C. Greiner, V. Schulze, A. Wanner, Study on micro texturing of uncoated cemented carbide cutting tools for wear improvement and built-up edge stabilisation, J. Mater. Process. Technol. 215 (2015) 62–70.
[7] S. Atlati, B. Haddag, M. Nouari, A. Moufki, Effect of the local friction and contact nature on the Built-Up Edge formation process in machining ductile metals, Tribology Int. 90 (2015) 217–227.
[8] T. Aiso, U. Wiklund, M. Kubota, S. Jacobson, Effect of Si and Cr additions to carbon steel on material transfer in a steel/TiN coated tool sliding contact, Tribology Int. 97 (2016) 337–348.
[9] T. Aiso, U. Wiklund, M. Kubota, S. Jacobson, Influence of Mn and Al additions to carbon steel on material transfer and coating damage mechanism in a sliding contact between steel and TiN coated HSS tool, Tribology Int. 101 (2016) 414–424.
[10] T. Aiso, U. Wiklund, M. Kubota, S. Jacobson, Effect of combined additions of Si, Mn, Cr and Al to carbon steel on material transfer in a steel/TiN coated tool sliding contact, in: Proceedings of the 17th Nordic Symposium on Tribology – 14–17 June, 2016 – Hämeenlinna, Finland, selected for publication in the NORDTRIB 2016 special issue of Wear.
[11] J. Gerth, J. Heinrichs, H. Nyberg, M. Larsson, U. Wiklund, Evaluation of an intermittent sliding test for reproducing work material transfer in milling operations, Tribology Int. 52 (2012) 153–160.
[12] E.M. Trent, P.K. Wright, Metal Cutting, 4th ed., Butterworth-Heinemann, Oxford, 2000.
[13] Handbook of Iron and Steel, 4th ed., (CD-ROM), The Iron and Steel Institute of Japan, 2002.
[14] E.M. Levin, C.R. Robbins, H.F. McMurdie, Phase Diagrams for Ceramists, I, The American ceramic society, USA, 1964.
[15] E.M. Levin, H.F. McMurdie, Phase Diagrams for Ceramists, III, The American ceramic society, USA, 1975.
[16] H. Yaguchi, K. Ozaki, M. Somekawa, Improvement of cutting tool life by AlN deposition on the tool, ISIJ Int. 44 (2004) 598–602.